Applications and Applied Mathematics: An International Journal (AAM)

Volume 19
Issue 3 *Special Issue No. 12 (March 2024)*

Article 7

3-2024

Utilization of Caputo Fractional Derivative in MHD Nanofluid Flow With Soret and Thermal Radiation Effects

Harshad Patel
Ganpat University

Gopal Nanda
Gujarat Technological University

Available at
http://pvamu.edu/aam
Appl. Appl. Math.
ISSN: 1932-9466

Applications and Applied Mathematics:
An International Journal
(AAM)

Special Issue No. 12 (March 2024), Article 7, 16 pages

Utilization of Caputo Fractional Derivative in MHD Nanofluid Flow With Soret and Thermal Radiation Effects

[1]Harshad Patel and [2*]Gopal Nanda

[1]U V Patel College of Engineering
Ganpat University
Kherva, Gujarat, India
harshadpatel2@gmail.com

[2*]Gujarat Technological University
Nigam Nagar, Chandkheda
Ahmedabad, India
gopalhnanda@gmail.com

*Corresponding Author

Received: May 1, 2023; Accepted: July 7, 2023

Abstract

In existence of heat diffusion and thermal radiation, an analytical equation is found for unsteady MHD flow past an exponentially accelerating vertical plate in optically thick water based nanofluid. The governing equations are made dimensionless by similarity transformation. A definition of Caputo fractional derivative is applied to generalize governing system of partial differential equations. Laplace transform techniques are applied and obtained the analytical solutions of proposed problems. For a physical point of view, numerical results are obtained using MATLAB software and presented via graphs. From the results, it is concluded that magnetic fields tend to reduce velocity. It is also worth noting that the heat transfer process improved with thermal radiation parameter whereas, mass transfer process improved with thermal diffusion.

Keywords: MHD; Nanofluid; Fractional derivative; Radiation; Diffusion; PDE; Unsteady flow

MSC 2020 No.: 76R50, 76W10, 76W05, 80A19, 80A21

Nomenclature

ρ_{nf}	Density of nanofluid (Kg m^{-3})
μ_{nf}	Dynamic viscosity of nanofluid (m^2s^{-1})
k_{nf}	Heat conductivity of nanofluid (W $m^{-1}k^{-1}$)
$(C_p)_{nf}$	Specific heat of nanofluid ($JKg^{-1}k$)
ϕ	Nanoparticle volume fraction
u	Fluid velocity in x −direction ($m\,s^{-1}$)
T	Temperature (k)
C	Concentration (Kg m^{-3})
g	Acceleration due to gravity ($m\,s^{-2}$)
D	Mass diffusivity (m^2s^{-1})
Nr	Thermal Radiation
Pr	Prandtl number
Gm	Mass Grashof number
Gr	Thermal Grashof number
t	Time(s)
Sc	Schmidt number
σ	Electric conductivity of the fluid ($m^{-1}s$)
$\beta_T{}'$	Volumetric coefficient of thermal expansion (k^{-1})
$\beta_C{}'$	Volumetric coefficient of concentration (m^3Kg^{-1})

1. Introduction

Magnetohydrodynamics is the science that investigates the interplay between magnetic and electrolytic fluids. The influence of magnetohydrodynamics is useful in the research of the human body's blood circulation system, the deformation of liquid into metal, plasma confinement, and a variety of other social and environmental concerns. Choudhury et al. (2018) discussed the Soret effect on MHD convective heat and mass transfer flow of an unsteady viscous incompressible electrically conducting fluid past a semi-infinite vertical porous plate in presence of chemical reaction and heat sink. Recently, Hossain et al. (2022) has discussed the Thermophysical characteristic of nanofluid in presence of magnetohydrodynamics. Saidulu et al. (2019) studied the condition of zero normal flux for tangent hyperbolic fluid over an inclined stretching sheet with the effects of radiation, heat source/sink and convective boundary condition. Bakar et al. (2021) linked the formation of a hybrid nanofluid in a porous media, heat production, thermal radiation, and magnetohydrodynamics to the behavior of flow and heat transmission on mixed convection (MHD). Kumar et al. (2016) investigated study the effects of diffusion-thermo and first order homogeneous chemical reaction on micropolar fluid flow over a vertical permeable plate in a porous medium.

Nanomaterials have far superior thermal, mechanical, optical, and transport qualities, making them an appealing research subject. Nanofluids are employed in a variety of industries including manufacturing, energy generation, and medicine. Hunegnaw and Demeke (2020) investigated the MHD mixed convective flow of Maxwell nanofluid past a porous vertically stretching sheet in the presence of chemical reaction. Nandi et al. (2021) examined the unsteady MHD free convective stagnation point flow of a hybrid nanofluid towards an exponentially stretched surface set in a uniform porous medium using ohmic, velocity slip, thermal radiation, and viscous dissipations. Sabu et al. (2021) examined the impacts of Soret effects, heat supply, and hall current on Magnetohydrodynamic convective ferro-nanofluid flow down an inclined channel with porous material on a theoretical and statistical level. Gopal and Kishan (2019) studied the viscous and Joule's dissipation on Casson fluid over a chemically reacting stretching sheet with inclined magnetic field and multiple slips. Kataria and Patel (2016) studied the impacts of heat and Soret production on Magnetohydrodynamic flow using an oscillatory vertical plate engrained in porous medium, whereas Kataria and Patel (2018) investigated the effect of heat exchange on Magnetohydrodynamic flow with soaring wall heat and increasing surface concentration.

Fractional calculus is an abstract concept that investigates non-integer order interpretations of differentiation. For a long time, it was thought to be just theoretically interesting. However, the emergence of various useful fractional derivative definitions has broadened the scope of its use. Over the past three decades, fractional calculus has progressed from a purely mathematical formulation to applications in biotechnology, shear modulus, biomechanics, physics, rheology, and electrodynamics. Fluids, biological systems' conductance, sound waves transmission, and data processing are few of the uses in science and technology. Aleem et al. (2020) studied how the Caputo fractional model may improve fluid flow, whereas Caputo-Fabrizio decays quicker than Caputo and is therefore ideally suited to displaying the memory of the flow problem at a certain moment. Ali et al. (2020) investigated the influence of copper oxide nanoparticles on the magnetohydrodynamic free convection transitory movement of a nano liquid on a vertical wall with time-dependent motion, heat, and intensity. Reyaz et al. (2022) have found an analytical solution for the Caputo-Fabrizio fractional derivative's actual impact on MHD flow in the presence of heat radiation and chemical reaction. In a magnetic and vibration environment, Maiti et al. (2021) built a fractional order plasma thermo - chemical flow structure that considered the Dufour and Soret effects. Recently, Upreti et al. (2022) studied Sisko fluid flow in stretching surface due to viscous dissipation and section whereas Upreti et al. (2020) and Upreti and Kumar (2020) considered radiation effects on MHD nanofluid flow.

Fractional calculus has recently drawn much interest in the domains of science and engineering. In literature, the fractional operator has been successfully used in numerous pieces. Studying the integrals and derivatives of different-order mechanisms is the focus of the rapidly expanding field of fractional calculus in mathematics. For the past few years, research on the concepts and traits of these fractional operators has increased significantly due to the high level of interest they have generated. It has proliferated among scientists working in various fields because of the positive precision obtained when several of the approaches in this calculus have been utilized to mimic some real-world phenomena (Kilbas et al. (2006); Magin (2004)). Recently, mathematicians, physicists, and engineers found fractional calculus a valuable concept in several disciplines, such as electrochemistry, rheology, quantitative biology, diffusion, etc. Caputo and Riemann-Liouville-related other fractional derivative operators are shown in Jarad, et al. (2012), Gambo et al. (2014), and Jarad et al. (2017).

2. Novelty of the Problem

Almost all engineering processes involve heat transfer and radiations. There are number of research articles dealing with thermal radiation. It is observed that work considering a coupled process by which solutes is transported in a medium under the action of a thermal gradient along with exponentially accelerated plate is limited. Also, efficiency of the system can be improved by taking nanofluids in the study. This motivated to this novel concept of considering Nanofluid Flow Past an Exponentially Accelerated Plate in presence of transverse magnetic field with Soret and Thermal Radiation.

3. Mathematical formulation

As illustrated in Figure 1, the flow is restricted to $y' > 0$, where y' is determined in direction normal to the plate. The fluid is deemed electrically conductive when a homogenous magnetic field B is supplied in a direction perpendicular to the plate.

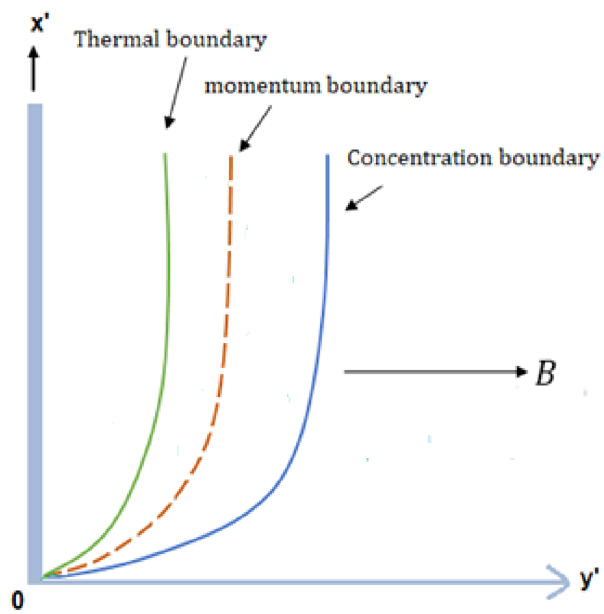

Figure 1. Physical Sketch of the Problem

The plate is already at rest with the ambient temperature T_0 at time $t' = 0$. The plate starts to swing at time $t' > 0$, according to $u_0 e^{at'}$, and the temperature of the plate is increased or decreased to T_w. The Rosseland approximation (1931) can be used to estimate radiative flux since nanofluid is optically thick. A radiative heat flow q_r is also expected to be applied to the plate in the normal direction. A medium is said to be optically thick if radiation exchange occurs and takes place only among neighboring volume elements. This is diffusion limit in which the governing radiative transport equations are differential equations. The water-based fluid and suspended nanoparticles copper or silver are also considered to be in thermal equilibrium, with density being proportional to temperature buoyancy forces. The governing momentum, energy and concentration equations are as follows.

$$\rho_{nf}\frac{\partial u'}{\partial t'} = \mu_{nf}\frac{\partial^2 u'}{\partial y'^2} - \sigma_{nf}B^2 u' + g(\rho\beta)_{nf}(T' - T_0) + g(\rho\beta_C)_{nf}(C' - C_0), \tag{1}$$

$$\frac{\partial T'}{\partial t'} = \frac{k_{nf}}{(\rho c_p)_{nf}}\frac{\partial^2 T'}{\partial y'^2} - \frac{\partial q_r}{\partial y'}, \tag{2}$$

$$\frac{\partial C'}{\partial t'} = D_C\frac{\partial^2 C'}{\partial y'^2} + D_T\frac{\partial^2 T'}{\partial y'^2}, \tag{3}$$

where

$$\rho_{nf} = (1-\emptyset)\rho_f + \emptyset\rho_s, \tag{4}$$

$$\mu_{nf} = \frac{\mu_f}{(1-\emptyset)^{2.5}}, \tag{5}$$

$$\sigma_{nf} = \sigma_f\left[1 + \frac{3(\sigma-1)\emptyset}{(\sigma+2)-(\sigma-1)\emptyset}\right], \tag{6}$$

$$\sigma = \frac{\sigma_s}{\sigma_f}, \tag{7}$$

$$(\rho\beta)_{nf} = (1-\emptyset)(\rho\beta)_f + \emptyset(\rho\beta)_s, \tag{8}$$

$$k_{nf} = k_f\left[1 - 3\frac{\emptyset(k_f-k_s)}{2k_f+k_s+\emptyset(k_f-k_s)}\right], \tag{9}$$

$$(\rho c_p)_{nf} = (1-\emptyset)(\rho c_p)_f + \emptyset(\rho c_p)_s, \tag{10}$$

$$q_r = -\frac{4\sigma^*}{3k^*}\frac{\partial T'^4}{\partial y'}. \tag{11}$$

By taking a suitably small temperature difference inside the flow, applying Taylor's series, and ignoring larger components, Equation (11) reduces to

$$q_r = -\frac{4\sigma^*}{3k^*}\frac{\partial(4{T_0}^3T' - 3{T_0}^4)}{\partial y'}. \tag{12}$$

Using Equation (12) in (2),

$$\left(\rho c_p\right)_{nf}\frac{\partial T'}{\partial t'}=\left(k_{nf}+\frac{16\sigma^* {T_0}^3}{3k^*}\right)\frac{\partial^2 T'}{\partial y'^2}\,, \tag{13}$$

with boundary conditions

$$u'=0, T'=T_0, C'=C_0;\ \text{as}\ y'\geq 0\ \text{and}\ t'=0,$$

$$u'=u_0e^{at'}, T'=T'_\infty+\left(T'_w-T'_\infty\right)t'/t_0\,, C'=C'_w\,,\ \text{as}\ t'\geq 0\ \text{and}\ y'=0,$$

$$u'\to 0, T'\to T_0, C'\to C_0;\ \text{as}\ y'\to\infty\ \text{and}\ t'\geq 0. \tag{14}$$

Introducing non-dimensional variables,

$$y=\frac{u_0y'}{v_f}, t=\frac{{u_0}^2t'}{v_f}, u=\frac{u'}{u_0}, \theta=\frac{T'-T_0}{T_w-T_0}, \omega=\frac{v_f\omega'}{{u_0}^2}, C=\frac{C'-C_0}{C_w-C_0}, \tag{15}$$

the system becomes:

$$\frac{\partial u}{\partial t}=a_1\frac{\partial^2 u}{\partial y^2}-a_3M^2u+a_2G_r\theta+G_ma_5C, \tag{16}$$

$$\frac{\partial \theta}{\partial t}=a_4\frac{\partial^2\theta}{\partial y^2}\,, \tag{17}$$

$$\frac{\partial C}{\partial t}=\frac{1}{S_c}\frac{\partial^2 C}{\partial y^2}+Sr\frac{\partial^2\theta}{\partial y^2}\,, \tag{18}$$

with initial and boundary conditions

$$u=0, T=T_0, C=C_0;\ \text{as}\ y\geq 0\ \text{and}\ t=0, \tag{19}$$

$$u=e^{at}\,, \theta=t\,, C=1, y=0, t>0, \tag{20}$$

$$u\to 0, \theta\to 0, C\to 0\ \text{as}\ y\to\infty, t>0, \tag{21}$$

where

$$Pr=\frac{\mu_f\left(\rho c_p\right)_f}{\rho_fk_f}\,, M=\frac{\sigma_fB^2v_f}{\rho_f{u_0}^2}\,, \frac{1}{k}=\frac{v_f\varphi^2}{k_1{u_0}^2}\,,\ Gr=\frac{g\beta_f(T_w-T_0)v_f}{{u_0}^3}\,,\ Sc=\frac{v_f}{D_C}\,,\ Kr=\frac{v_fk'}{{u_0}^2},$$

$$Gm = \frac{g\beta_c v_f (C_w - C_0)}{{u_0}^3}.$$

4. Solution of the problem

We apply the fractional derivative technique to generate analytical formulae for velocity, temperature, and concentration. We have used the Caputo fractional differential operator. Equations (16), (17), and (18) with the Caputo derivative have the following form:

$$D_t^{\propto}(u) = a_1 \frac{\partial^2 u}{\partial y^2} - a_3 M^2\, u(y,t) + a_2 Gr\, \theta(y,t) + Gm\, a_5 C(y,t), \tag{22}$$

$$D_t^{\beta}(\theta) = a_4 \frac{\partial^2 \theta}{\partial y^2}, \tag{23}$$

$$D_t^{\gamma}(C) = \frac{1}{Sc}\frac{\partial^2 C}{\partial y^2} + Sr \frac{\partial^2 \theta}{\partial y^2}, \tag{24}$$

where Caputo differential operator $D_t^{\propto}$ is defined as (Caputo 2015)

$$D_t^{\propto}(f(t)) = \frac{1}{\Gamma(1-\alpha)} \int_0^t \frac{f'(\tau)}{(t-\tau)^{\alpha}}\, d\tau \;;\; 0 < \alpha < 1,$$

where Γ is Gamma function.

4.1 Analytic Solution

The Laplace Transform and the Inverse Laplace Transform are used to find analytical solutions. Applying Laplace Transform to Equation (23) and using Laplace Transform of corresponding initial and boundary condition (19)-(21), we obtain

$$\bar{\theta}(y,q) = \frac{1}{q^2}\, e^{-\sqrt{\frac{q^{\beta}}{a_4}}\, y}, \tag{25}$$

where $\bar{\theta}(y,q)$ indicates the Laplace Transform of $\theta(y,t)$.

In order to obtain $\theta(y,t)$, we write Equation (25) in the form.

$$\bar{\theta}(y,q) = \frac{1}{q^2} \sum_{n=0}^{\infty} \frac{1}{n!}\left(-\frac{y}{\sqrt{a_4}}\right)^n q^{\frac{n\beta}{2}}. \tag{26}$$

Applying Inverse Laplace Transform to Equation (26), we get

$$\theta(y,t) = t \sum_{n=0}^{\infty} \frac{1}{n!\,\Gamma\left(2-\frac{n\beta}{2}\right)}\left(-\frac{y}{\sqrt{a_4 t^{\beta}}}\right)^n. \tag{27}$$

Now applying Laplace Transform to Equation (24) and using Laplace transform of corresponding initial and boundary condition (19)-(21), we obtain

$$\bar{C}(y,q) = \frac{1}{q}\, e^{-\sqrt{Sc\, q^{\gamma}}\, y} + \frac{ScSr\, q^{\beta-2}}{q^{\beta}-Sc\, a_4\, q^{\gamma}} \left\{ e^{-\sqrt{\frac{q^{\beta}}{a_4}}\, y} - e^{-\sqrt{Sc\, q^{\gamma}}\, y} \right\}. \tag{28}$$

Again, applying Laplace Transform to Equation (22) and using Laplace transform of corresponding initial and boundary condition (19)-(21), we obtain

$$\bar{u}(y,q) = A\, e^{-\sqrt{\frac{d_1+q^{\alpha}}{a_1}}\, y} - \frac{a_4\, d_2}{q^2[\, a_1\, q^{\beta}-a_4 d_1-a_4 q^{\alpha}]}\, e^{-\sqrt{\frac{q^{\beta}}{a_4}}\, y} - \frac{d_3}{q\, [a_1\, q^{\gamma} Sc-d_1-q^{\alpha}]}\, e^{-\sqrt{Sc\, q^{\gamma}}\, y}$$

$$-\frac{ScSr\, q^{\beta-2}\, d_3}{q^{\beta}-Sc\, a_4\, q^{\gamma}} \left\{ \frac{a_4\, e^{-\sqrt{\frac{q^{\beta}}{a_4}}\, y}}{a_1\, q^{\beta}-a_4 d_1-a_4 q^{\alpha}} - \frac{e^{-\sqrt{Sc\, q^{\gamma}}\, y}}{a_1\, q^{\gamma} Sc-d_1-q^{\alpha}} \right\}, \tag{29}$$

where

$$A = \frac{1}{q-a} + \frac{a_4\, d_2}{q^2[\, a_1\, q^{\beta}-a_4 d_1-a_4 q^{\alpha}]} + \frac{d_3}{q\, [a_1\, q^{\gamma} Sc-d_1-q^{\alpha}]} + \frac{ScSr\, q^{\beta-2}\, d_3}{q^{\beta}-Sc\, a_4\, q^{\gamma}} \left\{ \frac{a_4}{a_1\, q^{\beta}-a_4 d_1-a_4 q^{\alpha}} - \frac{1}{a_1\, q^{\gamma} Sc-d_1-q^{\alpha}} \right\}$$

$$d_1 = a_3 M^2\,,\ d_2 = a_2 Gr\,,\ d_3 = Gm\, a_5$$

For Equations (28) and (29), we can’t find the inverse Laplace transform analytically in the complex transformation domain. As a result, we employed numerical approaches to derive the inverse Laplace transform of Equations (28) and (29). In the numerical Laplace technique for solving fractional differential equations, Stehfest's (1970) and Tzou's (1970) algorithms are utilized.

4.2 Nusselt Number and Sherwood Number

The Nusselt number Nu and Sherwood Number Sh can be expressed as

$$Nu = -\left(\frac{\partial\theta}{\partial y}\right)_{y=0} \ \&\ Sh = -\left(\frac{\partial C}{\partial y}\right)_{y=0}. \tag{30}$$

4.3 Numerical Solution

The governing linear parabolic partial differential equations (16)-(18) with initial and boundary conditions are solved numerically by using MATLAB software (PDEPE Solver). We have taken increment step along t as 0.09090 and y directions as 0.09677 in entire numerical computations. In present problem, the cost and the accuracy of the solution depend strongly on length of the vector y. This attentive problem requests the solution on mesh produced by spaced points from the spatial interval 31 values of y from the space interval [0, 3] and 11 values of t from the time interval [0, 1].

5. Results and Discussion

The physical interpretation of the observed data is presented in this part, which includes graphs. Numerical simulations were carried out to demonstrate the impact of various physical characteristics. The following are the results that we obtained to demonstrate the impacts of nanoparticle volume fraction $\emptyset$, magnetic field parameter M, Thermal Radiation number Nr, Prandtl number Pr, Schmidt number Sc, Mass Grashof number Gm, Thermal Grashof number Gr, and Soret number Sr on Momentum, Heat and Diffusion profiles.

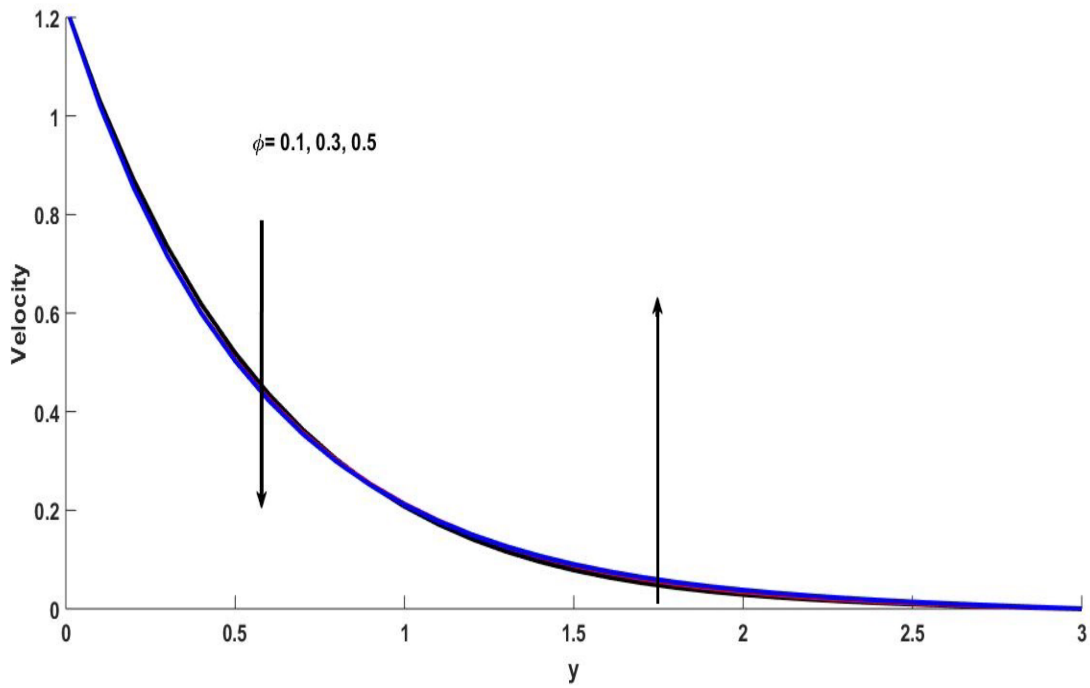

Figure 2. Velocity profile u for distinct values of $\emptyset$

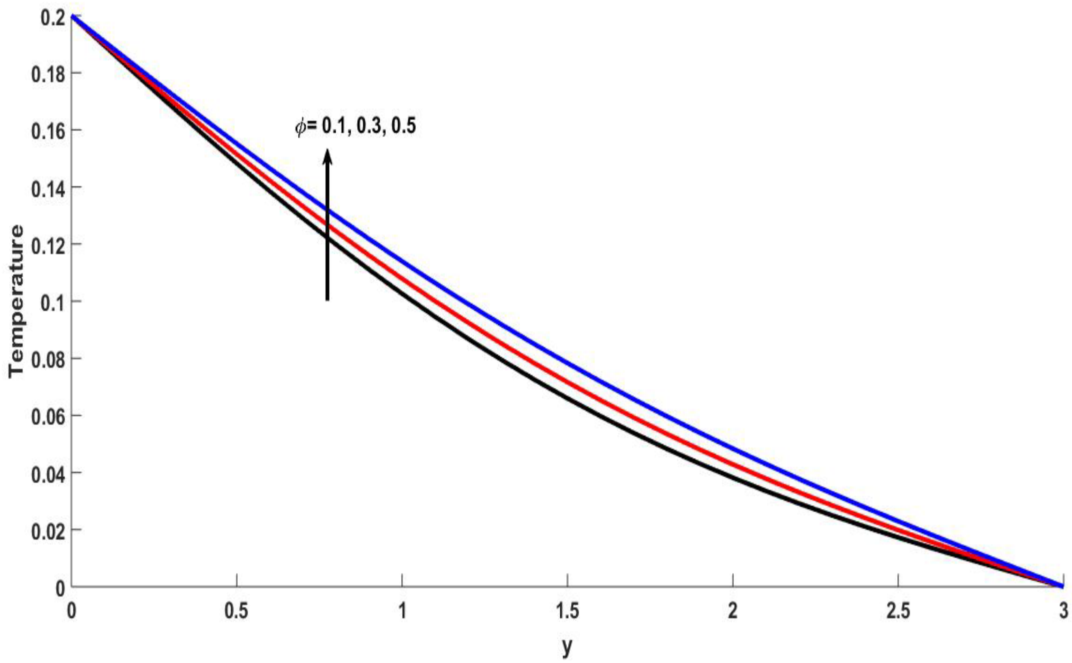

Figure 3. Temperature profile θ for distinct values of $\emptyset$

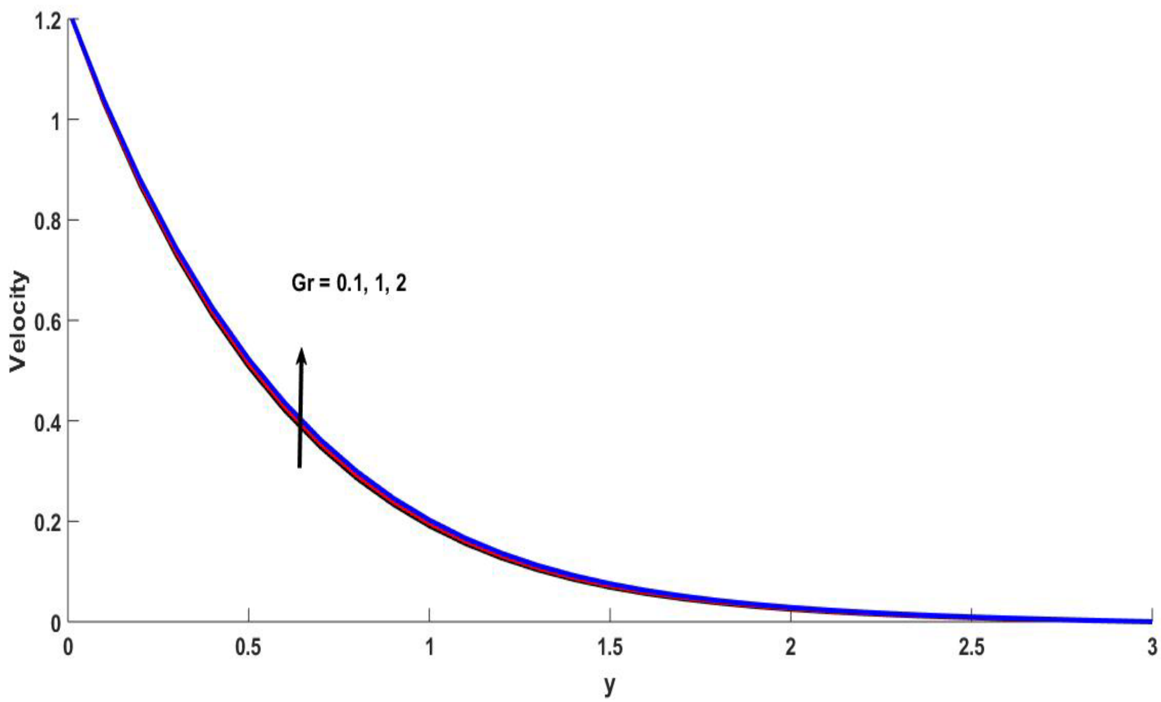

Figure 4. Velocity profile u for distinct values of Gr

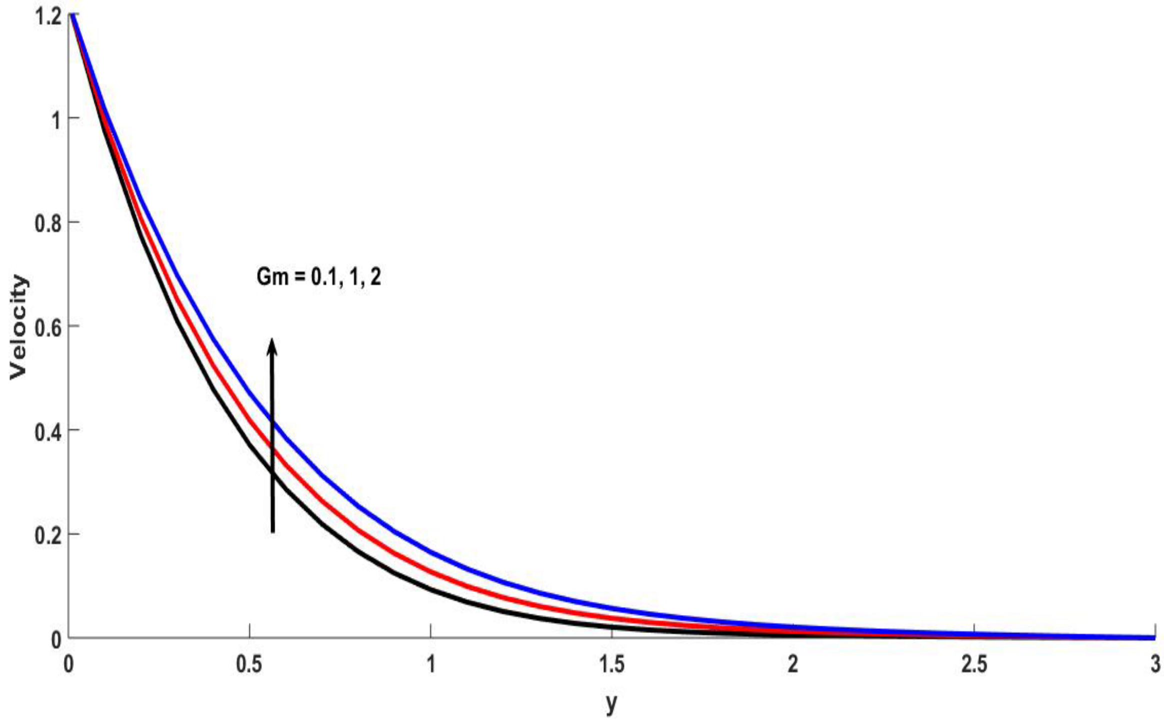

Figure 5. Velocity profile u for distinct values of Gm

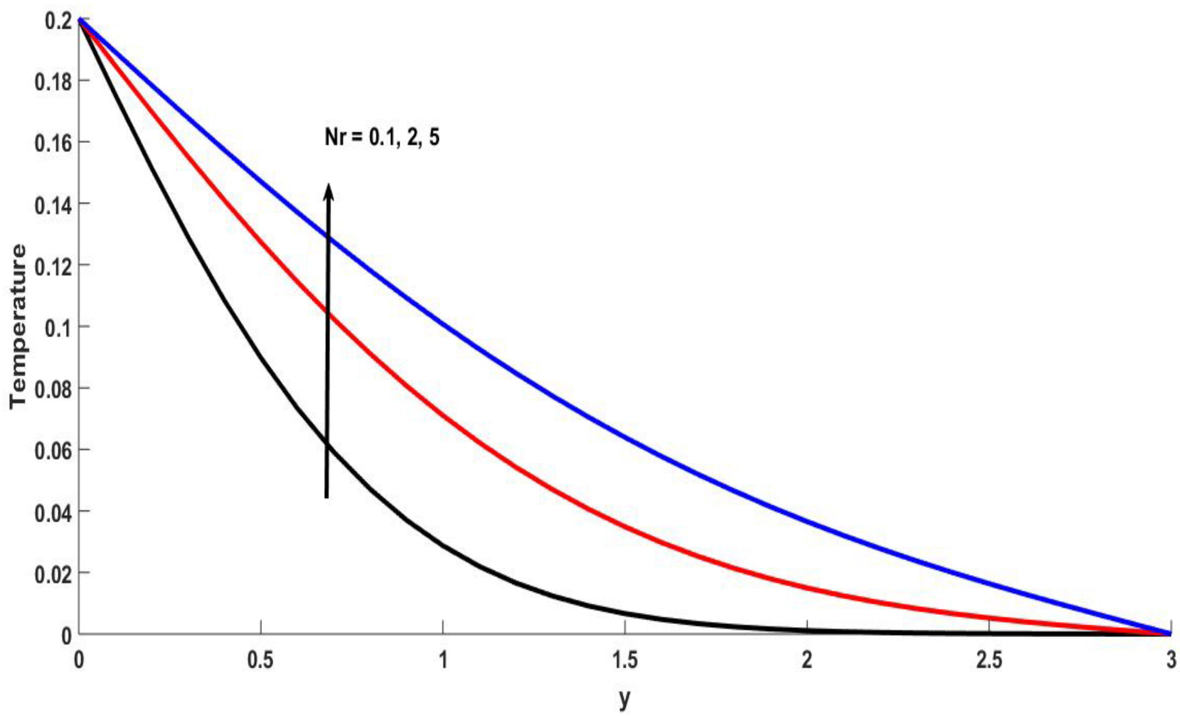

Figure 6. Temperature profile θ for distinct values of Nr

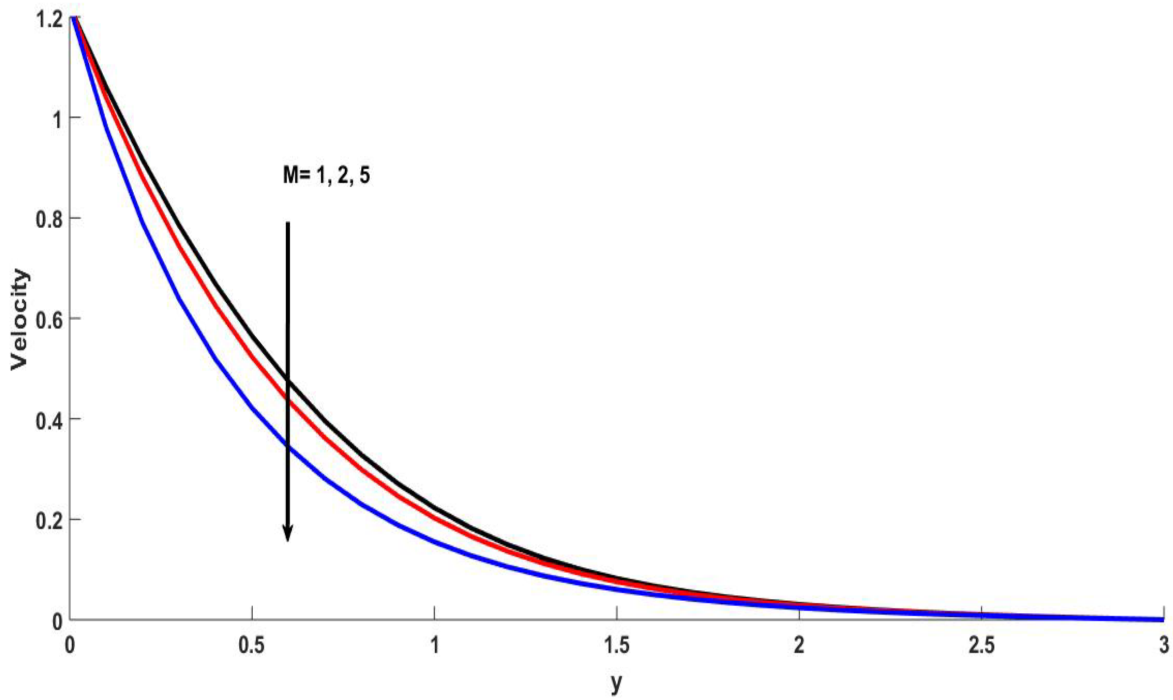

Figure 7. Velocity profile u for distinct values of M

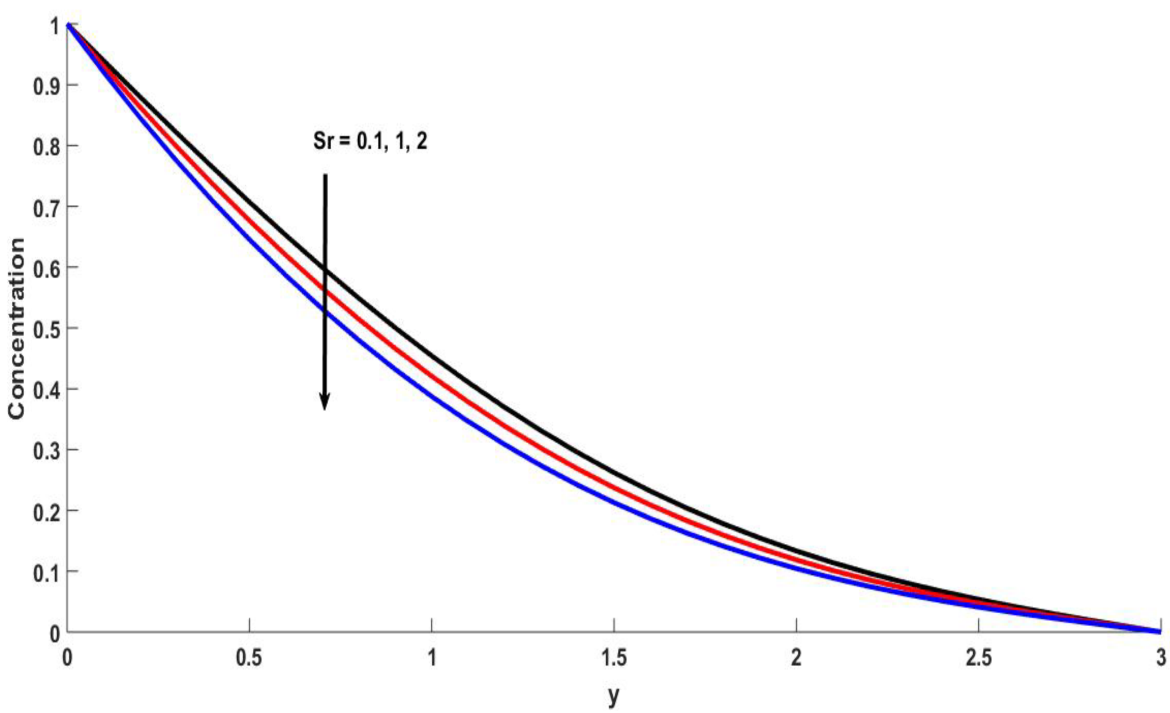

Figure 8. Concentration profile C for distinct values of Sr

Table 1: Comparison of Sherwood Number with Patel et al. (2022) at $Sr = 0$

Sc	t	Patel et al. (2022)	Present Study
1.5	0.4	-0.2185	-0.2185
2.0	0.4	-0.2523	-0.2523
2.5	0.4	-0.2821	-0.2821
1.5	0.5	-0.2443	-0.2443
1.5	0.6	-0.2676	-0.2676

The influence of nanoparticle volume fraction $\emptyset$ on fluid momentum is depicted in Figure 2. In Figure 2, as the value $\emptyset$ rises, the fluid momentum slows down in the interval (0,1) and fluid velocity increases in the interval (1,3). Figure 3 depicts the volume fraction as a function of temperature. The fluid temperature rises as $\emptyset$ increases, which can be seen in the graph. It is because when the value of nanoparticle volume fraction $\emptyset$ grows, the viscous forces increase, causing the heat capacity of the fluid to rise, resulting in a rise in temperature. The influence of Thermal Grashof number *Gr* and Mass Grashof number *Gm* have been displayed in Figure 4 and Figure 5. As illustrated in both images, higher *Gm* and *Gr* values increase the fluid momentum. It's because of the proportions of buoyancy and viscous forces. As a result, raising the values of *Gr* and *Gm* lowers viscosity by increasing the buoyancy force. The influence of the radiation parameter *Nr* on the heat profile is seen in Figure 6. Higher levels of *Nr* result in a rise in temperature, as shown in the graph. The temperature effect of *Nr* is consistent with its physical behavior, resulting in a rise in nanofluid temperature in the boundary layer area. Figure 7 shows the momentum of a fluid as a function of the magnetohydrodynamic (MHD) parameter, *M*. The existence of a magnetic material or even an electrical current that produces magnetic fields could trigger the induced magnetic field. The magnetic field's pulling force grows as the MHD parameter is enhanced. The fluid flow is hindered as a result, and the fluid motion is lowered. The cause of Soret number *Sr* on concentration profile has been illustrated in Figure 8 and it has been observed that concentration profile decreases as Soret number *Sr* rises. Table 1 communicates the comparison of rate of mass transfer with the analysis reported by Patel et al. (2022). It demonstrates the validity of the current study by comparing it to previous findings; this indicates they are in good agreement. It supports our findings in terms of Sherwood number since it agrees well with the previously stated results.

6. Conclusion

Stable MHD flow through an exponentially accelerating vertical surface in optically thick nanofluid has been examined in the influence of heat transfer and thermal radiation. Closed form issues are solved using the Laplace technique and the Caputo fractional model. The impact of various factors on velocity profile, temperature profile, and concentration profile has been studied through graphs. The current investigation yielded the following key findings.

- The Mass Grashof number and Thermal Grashof numbers tend to accelerate the motion of fluid flow.
- The fluid motion reduced by increasing the value of nanoparticle volume fraction, Magnetic field.
- The heat transfer enhanced with nanoparticle volume fraction and Thermal Radiation parameter.
- Thermo-diffusion tends to reduce the mass transfer process.

References

Aleem, M., Asjad, M. I., Shaheen, A. and Khan, I. (2020). MHD Influence on different water based nanofluids (TiO2, Al2O3, CuO) in porous medium with chemical reaction and newtonian heating, Chaos, Solitons & Fractals, Vol. 130. http://doi.org/10.1016/j.chaos.2019.109437

Ali, F., Ali, F., Sheikh, N.A. and Khan, I. and Nisar, K.S. (2020). Caputo–Fabrizio fractional derivatives modeling of transient MHD Brinkman nanoliquid: Applications in food technology, Chaos, Solitons & Fractals, Volume 131. https://doi.org/10.1016/j.chaos.2019.109489

Bakar, S.A., Norihan, M.A., Bachok, N. and Ali, F. (2021). Effect of thermal radiation and MHD on hybrid Ag–TiO2/H2O nanofluid past a permeable porous medium with heat generation, Case Studies in Thermal Engineering, Volume 28. https://doi.org/10.1016/j.csite.2021.101681

Caputo, M. and Fabrizio, M. (2015). A new definition of fractional derivative without singular kernel, Progr Fract Differ Appl, Vol. 1, No. 2, pp. 1-13.

Choudhury, K. and Ahmed, N. (2018). Soret Effect on Transient MHD Convective Flow past a Semi-infinite Vertical Porous Plate with Heat Sink and Chemical Reaction, Applications and Applied Mathematics, Vol. 13, Issue 2, pp. 839 – 853.

Gambo, Y. Y., Jarad, F., Baleanu, D. and Abdeljawad, T. (2014). On Caputo modification of the Hadamard fractional derivatives, Advances in Difference Equations, Vol. 10, pp. 1-12.

Gopal, D. and Kishan, N. (2019). Brownian Motion and Thermophoresis Effects on Casson Nanofluid Over a Chemically Reacting Stretching Sheet with Inclined Magnetic Field, Applications and Applied Mathematics, Vol. 14, Special Issue No. 4, pp. 106 – 116.

Hossain, R., Azad, A.K., Hasan, M.J. and Rahman, M.M. (2022). Thermophysical properties of Kerosene oil-based CNT nanofluid on unsteady mixed convection with MHD and radiative heat flux, Engineering Science and Technology, an International Journal, Vol. 35. https://doi.org/10.1016/j.jestch.2022.101095

Hunegnaw, D. and Demeke, F. (2020). MHD Mixed Convective Flow of Maxwell Nanofluid Past a Porous Vertical Stretching Sheet in Presence of Chemical Reaction, Applications and Applied Mathematics, Vol. 15, Issue 1, pp. 530 – 549.

Jarad, F., Abdeljawad, T. and Baleanu, D. (2012). Caputo-type modification of the Hadamard fractional derivatives, Advances in Difference Equations, Vol. 142, pp. 1-8.

Jarad, F., Abdeljawad, T. and Baleanu, D. (2017). On the generalized fractional derivatives and their Caputo modification, Vol. 10, No. 5, pp. 2607-2619.

Kataria, H.R. and Patel, H. R. (2016). Radiation and chemical reaction effects on MHD Casson fluid flow past an oscillating vertical plate embedded in porous medium, Alexandria Engineering Journal, Vol. 55, pp. 583-595.

Kataria, H.R. and Patel, H. R. (2016). Soret and heat generation effects on MHD Casson fluid flow past an oscillating vertical plate embedded through porous medium, Alexandria Engineering Journal, Vol. 55, pp. 2125-2137.

Kataria, H.R. and Patel, H. R. (2018). Effect of thermo-diffusion and parabolic motion on MHD Second grade fluid flow with ramped wall temperature and ramped surface concentration, Alexandria Engineering Journal, Vol. 57, No. 1, pp. 73-85.

Kilbas, A., Srivastava, H.M. and Trujillo, J.J. (2006). *Theory and Applications of Fractional Differential Equations*, Volume 204.

Kumar, K., R.V.M.S.S, Raju, V.C.C., Durga Prasad, P. and Varma, S.V.K. (2016). Heat and Mass Transfer in MHD Micropolar Fluid in The Presence of Diffusion Thermo and Chemical Reaction, Applications and Applied Mathematics, Vol. 11, Issue 2, pp. 704 – 721.

Magin, R.L. (2004). Fractional calculus in bioengineering, Critical Reviews in Biomedical Engineering, Vol. 32, No. 1. DOI:10.1615/CritRevBiomedEng.v32.i1.10

Maiti, S., Shaw, S. and Shit, G.C. (2021). Fractional order model for thermochemical flow of blood with Dufour and Soret effects under magnetic and vibration environment, Colloids and Surfaces B: Biointerfaces. Vol. 197. https://doi.org/10.1016/j.colsurfb.2020.111395

Nandi, S., Kumbhakar, B. and Seth, G. S. (2021). Quadratic regression analysis of unsteady MHD free convective and radiative-dissipative stagnation flow of hybrid nanofluid over an exponentially stretching surface under porous medium, Chin. J. Phys., Vol. 77, pp. 2090-2105.

Patel, H., Mittal, A. and Nagar, T. (2022). Fractional order simulation for unsteady MHD nanofluid flow in porous medium with Soret and heat generation effects, Heat Transfer, Vol. 52. https://doi.org/10.1002/htj.22707

Reyaz, R., Mohamad, A. Q., Lim, Y. J., Saqib, M. and Shafie, S. (2022). Analytical Solution for Impact of Caputo-Fabrizio Fractional Derivative on MHD Casson Fluid with Thermal Radiation and Chemical Reaction Effects, Fractal Fract., Vol. 6, No. 1, https://doi.org/10.3390/fractalfract6010038

Rosseland, S. (1931). *Astrophysik und atom-theoretische Grundlagen*, Springer-Verlag, Berlin. https://doi.org/10.1007/978-3-662-26679-3

Sabu, A. S., Mathew, A., Neethu, T. S. and George, K.A. (2021). Statistical analysis of MHD convective ferro-nanofluid flow through an inclined channel with hall current, heat source and Soret effect, Thermal Science and Engineering Progress, Volume 22. https://doi.org/10.1016/j.tsep.2020.100816

Saidulu, N., Gangaiah, T. and Venkata Lakshmi, A. (2019). MHD Flow of Tangent Hyperbolic Nanofluid over an Inclined Sheet with Effects of Thermal Radiation and Heat Source/Sink, Applications and Applied Mathematics, Vol. 14, Special Issue No. 4, pp. 54 – 68.

Stehfest. H. (1970). Algorithm 368, Numerical inversion of Laplace Transform, Commun ACM, Vol. 13, No. 1, pp. 47-49.

Tzou. D. (1970). *Macro to Microscale Heat Transfer: The Behavior*, Taylor and Francis, Washington.

Upreti, H., Joshi, N., Pandey, A. K. and Rawat, S. K. (2022). Assessment of Convective Heat Transfer in Sisko Fluid Flow via Stretching Surface Due to Viscous Dissipation and Suction, Nanoscience and Technology: An International Journal, Vol. 13, No. 2, pp. 31-44.

Upreti, H. and Kumar, M. (2020). Influence of non-linear radiation, Joule heating and viscous dissipation on the boundary layer flow of MHD nanofluid flow over a thin moving needle, Multidiscipline Modeling in Materials and Structures, Vol. 16, No. 1, pp. 208-224.

Upreti, H., Rawat, S.K. and Kumar, M. (2020). Radiation and non-uniform heat sink/source effects on 2D MHD flow of CNTs-H_2O nanofluid over a flat porous plate, Multidiscipline Modeling in Materials and Structures, Vol. 16, No. 4, pp. 791-809.

Appendix

$b_0 = 1 - \emptyset,$	$b_1 = (b_0 + \emptyset \frac{\rho_s}{\rho_f})$	$b_2 = (b_0 + \emptyset \frac{(\rho\beta)_s}{(\rho\beta)_f})$
$b_3 = (b_0 + \emptyset \frac{(\rho c_p)_s}{(\rho c_p)_f}),$	$b_4 = \frac{k_{nf}}{k_f},$	$b_5 = \frac{\sigma_{nf}}{\sigma_f},$
$b_6 = \frac{b_4}{b_3},$	$b_7 = (b_0 + \emptyset \frac{(\rho\beta)_c}{(\rho\beta)_f}),$	$a_1 = \frac{1}{{b_0}^{2.5} b_1}$
$a_2 = \frac{b_2}{b_1}$	$a_3 = \frac{b_5}{b_1}$	$a_4 = \frac{b_4 + Nr}{b_3 pr}$
$a_5 = \frac{b_7}{b_1},$	$H = a_1 b_6$	